

## Supplementary material

### Supplementary Materials and Methods

#### HTS

STF cells were seeded in 384-well plates (Corning) at 2500 cells/well density using Multidrop Combi dispenser (Thermo Scientific) and cultured overnight. The next day, mouse recombinant Wnt3a was added together with the tested compound (final concentration 1  $\mu$ M) using pintool (V&P Scientific) coupled to a JANUS Automated Workstation (PerkinElmer). The cells were cultured for additional 24 h, lysed directly in the well, and the luciferase activity was determined.

#### Plasmid constructs

Constructs encoding FLAG-tagged (N-terminus) human wt  $\beta$ -CATENIN and S45A and  $\Delta$ S45 variants were generated by PCR and cloned into the pTripleFLAG-C3 mammalian expression vector. Constructs encoding the  $\beta$ -CATENIN variants S33Y, S37A and  $\Delta$ N (the N-terminal deletion encompassed amino acids 1-131) generated in expression vectors pCS2 and pcDNA3.1 (Invitrogen) were kindly provided by T. Valenta. The Lef1-VP16 construct encoding the N-terminally truncated mouse Lef1 (an internal Bgl II restriction enzyme recognition site was utilized for cloning) fused to the C-terminal transcription transactivation domain of the herpes simplex virus protein VP16 was generated in the pK-Myc vector (1); HA-CBP was obtained from Addgene (#32908). The expression construct encoding the N-terminally truncated human LRP6 ( $\Delta$ N-LRP6) was a kind gift from V. Bryja.

#### Antibodies

These mouse monoclonal antibodies were used for immunocytochemistry and immunohistochemistry: anti- $\beta$ -catenin (clone E-5, Santa Cruz; #14, BD Transduction Laboratories; EM-22, Exbio), anti-Ki67 (Mob 237, Diagnostic BioSystems), anti-Krt20 (K<sub>s</sub> 20.8, Dako), anti-p21 (SXM30, BD Pharmingen), anti-PCNA (rabbit polyclonal, Abcam). These antibodies were used for immunoblotting: anti- $\alpha$ -tubulin (mouse monoclonal, TU-01, Exbio), anti- $\beta$ -catenin (mouse monoclonal, EM-22, Exbio), anti-non-phospho- $\beta$ -catenin/S33/S37/T41 (rabbit polyclonal, Cell Signaling), anti-phospho- $\beta$ -catenin/Ser675 (rabbit polyclonal, Cell Signaling), anti-acetylated-lysine (rabbit monoclonal, #9814, Cell Signaling), anti-Axin2 (rabbit monoclonal, 76G6, Cell Signaling),

anti-Flag (mouse monoclonal, M2, Sigma), anti-HA tag (mouse monoclonal, 12CA5, Abcam), anti-Tcf4 (rabbit monoclonal, C48H11, Cell Signaling), anti-LRP6 (rabbit monoclonal, C5C7, Cell Signaling), anti-phospho-LRP6/Ser1490 (rabbit polyclonal, Cell Signaling).

#### **Densitometric analysis of western blots**

Protein levels were quantified using GS-800 Calibrated Densitometer and Quantity One software (Bio-Rad).

#### **Cell cycle analysis**

SW480 and HCT116 CRC cells were fixed by 70% ethanol and stained using propidium iodide (Sigma; final concentration 20  $\mu$ g/ml). Cell fluorescence was acquired using LSR II flow cytometer (BD Biosciences). Cells were stained with Hoechst 33342 (Invitrogen) to discriminate G2 cells and cell doublets.

#### **Quantification of proliferating cells in tissue sections**

Tissue sections obtained from monensin- or vehicle-treated mice were incubated with an anti-PCNA antibody, washed and stained using the Alexa 488 dye conjugated to a goat anti-rabbit antibody (Molecular Probes) and DAPI (Sigma) nuclear stain. Ten fluorescent microscopy images were taken from five animals in each group. The PCNA and DAPI fluorescent signal in tumors was analyzed using the ImageJ software.

#### **ROS measurement**

The carboxy derivative of fluorescein (carboxy- $H_2$ DCFDA; Molecular Probes) was utilized for ROS detection. Cells were seeded at the density of 20,000 cells/well of a black 96-well plate. Cells were incubated with the carboxy- $H_2$ DCFDA probe dissolved in culture medium (final concentration 100  $\mu$ M) at 37°C for 50 min. Cells were washed twice with PBS and incubated with monensin or vehicle (DMSO). Hydrogen peroxide was used as a positive control. Probe oxidation measurement started immediately after monensin/DMSO addition and continued every 6 minutes for 2 hours (at 37°C) using EnVision Multilabel Plate Reader. For each type of treatment, the average value of fluorescence with standard deviation was determined from six wells.

#### **Disruption of the *APC* gene using TALENs**

Constructs encoding one pair of TALENs targeting the human *APC* gene was purchased from TALEN Library Resources (H1458; Seoul National University, Korea). The TALEN recognition sequences are given in Supplementary Fig. S2. The TALEN constructs were co-transfected with EYFP-producing plasmid (pEYFP-N3; Clontech) into STF cells; the next day single EYFP-positive

cells were sorted and expanded. Genomic DNA isolated from individual cell clones was used to identify cells harboring modified *APC* alleles. First, the DNA fragment amplified from genomic DNA by primers hAPC TALEN test F 5' GGCTGCGGTGAAAGCTATGATCATTCC 3' and hAPC TALEN test R 5' GATAACAGAAGTTGGTGGCCTTATATCC 3' (fragment length obtained from the wt APC allele: 684 bp) was digested using the Bgl II restriction endonuclease. Subsequently, DNA fragments isolated from six cell clones that were uncut (clones numbers: 1, 3, and 5) or partially cut (2, 4, 6) by the enzyme were cloned into the pGEM-T Easy vector (Promega) and sequenced.

### **LC-MS/MS and protein kinase selectivity profiling**

LC-MS/MS was performed using anti- $\beta$ -catenin precipitates obtained from monensin-treated (5  $\mu$ M) or control (DMSO) SW480 and HCT116 cells. After reduction and alkylation, precipitates were subjected to trypsin (Promega) digestion. The aliquot of each sample (1/100) was directly analyzed by LC-MS/MS for protein identification. Another part of sample (1/3) was subjected to phosphopeptide analysis. Phosphopeptides were enriched using TiO<sub>2</sub> kit (Thermo Fisher Scientific). Eluates were concentrated under vacuum and then diluted in 10  $\mu$ l of 0.1% FA solution before the analysis. LC-MS/MS analysis was performed using reverse phase RSLCnano system (Dionex) on-line coupled with an Orbitrap Elite hybrid spectrometer (Thermo Fisher Scientific). The analysis of the mass spectrometric data files was carried out using the Proteome Discoverer software (version 1.3) with in-house Mascot search engine utility. Mascot MS/MS ion searches were done against NCBI protein database (taxonomy Mammalia). PhosphoRS feature was used for phosphorylation localization (2). Kinase profiling was performed at the International Centre for Protein Kinase Profiling, MRC, Dundee, UK.

## Supplementary References

1. Valenta T, Lukas J, Korinek V. HMG box transcription factor TCF-4's interaction with CtBP1 controls the expression of the Wnt target Axin2/Conductin in human embryonic kidney cells. *Nucleic Acids Res.* 2003;31:2369-80.
2. Taus T, Kocher T, Pichler P, Paschke C, Schmidt A, Henrich C, et al. Universal and confident phosphorylation site localization using phosphoRS. *J Proteome Res.* 2011;10:5354-62.
3. Park YW, Cummings RT, Wu L, Zheng S, Cameron PM, Woods A, et al. Homogeneous proximity tyrosine kinase assays: scintillation proximity assay versus homogeneous time-resolved fluorescence. *Anal Biochem.* 1999;269:94-104.

## Supplementary Figure Legends

**Supplementary Figure S1.** Densitometric analysis of western blots shown in Figs. 2D (A), 3C (B) and 4D (C). The diagrams represent the average optical density (OD) of detected bands. Values obtained in cells treated with vehicle (DMSO) were set to 100%. The level of the individual protein (or the protein form) was normalized to the  $\alpha$ -TUBULIN signal. Error bars represent SDs.

**Supplementary Figure S2.** Monensin suppresses Wnt signaling activated by TALEN-induced disruption of the *APC* gene. A, luciferase reporter assay in parental STF cells and six cellular clones with one (clones 2, 4, 6) or both alleles (clones 1, 3, 5) of *APC* disrupted by TALENs. B, immunoblotting of cell lysates obtained from indicated clones illustrate an increase in the total  $\beta$ -catenin level in *APC*-deficient cells. C, DNA (top) and protein (bottom) sequences of the TALEN-targeted region and allelic changes found in clone 1. Numbers indicate the positions in the translated portion of *APC* cDNA or protein. TALEN-mediated cut and subsequent repair of genomic DNA generates 28 and 14 nucleotide deletions in the coding sequence resulting in a premature stop of translation. Amino acid residues translated upon the frameshift are shown in red; asterisks indicate premature termini of the protein. D, monensin blocks Wnt signaling in *APC*-deficient STF cells. Results of the luciferase reporter assay performed in clone 1 cells treated with monensin or DMSO. The average luciferase units were corrected for the cell viability using Cell Titer Blue fluorescent measurement; error bars, SDs; \*\* $P < 0.01$ .

**Supplementary Figure S3.** Monensin does not interfere with Dvl phosphorylation. Immunoblotting of whole-cell extracts prepared from 3T3 cells treated with Wnt3a and monensin as indicated. The putative phosphorylated form of Dvl with changed mobility in the gel is marked by arrow. Cell extract obtained from cells treated with CK1 $\epsilon$  inhibitor PF670462 (Sigma) was analyzed in the very right lane.

**Supplementary Figure S4.** The inhibitory effect of monensin on Wnt signaling is not restricted to the vesicular acidity blockade. The Wnt pathway was activated in STF using recombinant Wnt3a ligand (A), cell transduction with lentivirus expressing Wnt1 (B), transfection with the construct producing N-terminally truncated Wnt co-receptor LRP6 ( $\Delta$ N-LRP6) (C) and transient transfection with the construct encoding wt  $\beta$ -CATENIN (D). Luciferase activity was determined after overnight treatment with monensin, endosomal acidification inhibitor bafilomycin A or DMSO. The average RLU/s of the triplicate were corrected for cell viability or transfection efficiency using the Cell Titer-Blue Cell

Viability Assay Kit (A, B) or Renilla luciferase construct (C, D). The Wnt pathway activity in cells treated with vehicle was arbitrarily set to 100%. Error bars represent SDs; \*\* $P < 0.01$ .

**Supplementary Figure S5.** Monensin inhibits aberrant Wnt signaling in CRC cells COLO320 and LS174T. A, *APC*-deficient COLO320 cells and LS174T cells harboring oncogenic mutation in  $\beta$ -catenin were treated either with vehicle alone (DMSO) or monensin for 36 h before analysis. The diagrams depict the results of qRT-PCR analysis of the TCF/ $\beta$ -catenin target gene expression. The expression level of the given gene in unstimulated cells was arbitrarily set to 1. The amount of input cDNA was normalized to the *UBB* gene. The experiment was repeated twice in triplicates; error bars indicate SDs. Corresponding CT values are shown in Supplementary Table S4. Notice that the expression level of the Wnt target gene *LGR5* was evaluated in LST174 cells only, since the gene is not produced in other CRC cells. B, fluorescent microscopy images of COLO320 and LS174T cells treated either with DMSO or monensin for 36 h. In the merged images the  $\beta$ -catenin staining is depicted in green, cell nuclei were stained using DAPI stain (blue); original magnification: 400 $\times$ . C, Western blot analysis of COLO320 and LS174T cells incubated for 36 h with vehicle or monensin. Densitometric analysis of the western blots is given at the right. D, monensin suppresses cell proliferation of COLO320 and LS174T cells.  $^3\text{H}$ -thymidine incorporation into genomic DNA of cells treated with vehicle or monensin. The diagram depicts the mean values of four biological replicates with error bars indicating SDs; the  $^3\text{H}$ -thymidine counts in control cells (treated with vehicle only) was arbitrarily set to 100%.

**Supplementary Figure S6.** ROS concentration is not increased by monensin. HEK293 and SW480 cells were incubated with the carboxy- $\text{H}_2\text{DCFDA}$  ROS probe and treated with the indicated concentrations of monensin or vehicle (DMSO). Cells treated with hydrogen peroxide were used as a positive control. Florescence of the oxidized probe was determined in 6-minute intervals. The diagrams represent average values of fluorescent units (FUs) obtained from six wells; error bars, SDs.

**Supplementary Figure S7.** Membranous localization of  $\beta$ -catenin in HCT116 cells. Confocal microscopy images of SW480, LS174T and HCT116 cells stained with the indicated anti- $\beta$ -catenin antibodies.

**Supplementary Figure S8.** Monensin does not inhibit  $\beta$ -catenin acetylation. HEK293 cells were co-transfected with constructs encoding HA-tagged acetylase CREB binding protein (HA-CBP) and

FLAG-tagged  $\beta$ -catenin. Beta-catenin was immunoprecipitated and its acetylation detected on the western blots using an anti-acetyl-lysine antibody. IP, immunoprecipitation; acetylated proteins non-specifically associated with Sepharose beads are indicated by red asterisk.

**Supplementary Figure S9.** Monensin does not change the fraction of proliferating cells in intestinal tumors. A, hematoxylin and anti-PCNA-stained sections of the jejunum of APC<sup>+/Min</sup> mice treated with monensin or vehicle (DMSO). B, microscopic images showing the PCNA fluorescent signal in green and DAPI signal in blue. C, estimated cell proliferation in the tumors. Diagram represents the ratio of the PCNA to DAPI florescent signal in tumor tissue derived from monensin-treated or control mice; error bars, SDs. Bar: 0.2 mm (a, b); 0.1 mm (c, d, e, f); 0.066 mm (a', b'); 0.05 mm (c', d', e', f').

## Supplementary Table Legends

**Supplementary Table S1.** Sequences of primers used for qRT-PCR analyses. The sequence of the forward primer is given in the upper line with the corresponding reverse primer in the lower line.

**Supplementary Table S2.** Monensin does not inhibit enzymatic activity of any of the tested protein kinases. The compound was profiled against a panel of 50 different kinases at a concentration of 0.1 and 1  $\mu$ M; the quantification employed radioactive  $^{33}\text{P}$ -ATP filter-binding assay (3). The data is presented as the remaining kinase activity in % at a given concentration of monensin in duplicate assays, and compared with DMSO controls. The profiling revealed that monensin did not inhibit enzymatic activity of any of the tested kinases below 60%, and the result was therefore considered to be negative.

**Supplementary Table S3.** qRT-PCR analysis of the TCF/ $\beta$ -catenin target gene expression in CRC cells. Cells were treated with DMSO (vehicle) or monensin 36 h before harvesting. The average CT values for the given gene normalized to *UBB* expression (CT value was arbitrarily set to 19) are shown. The experiment was performed in triplicates; corresponding diagrams (including SDs) are shown in Fig. 4B and Supplementary Fig. S5A.

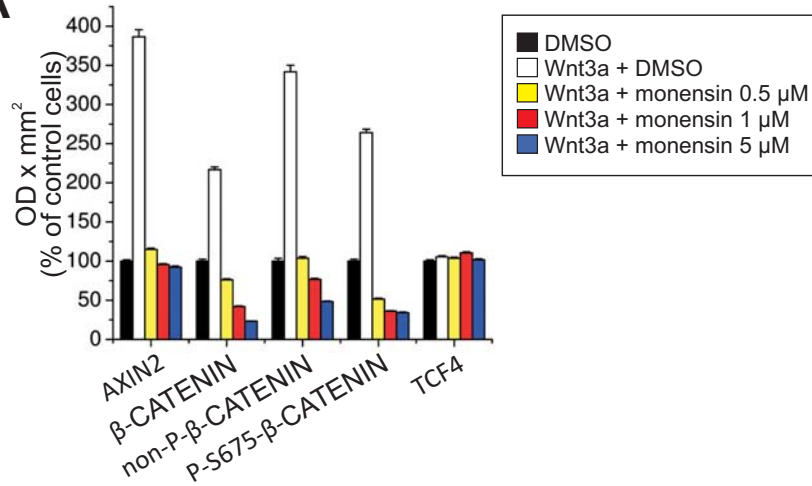
**Supplementary Table S4.** Cell cycle analysis of SW480 and HCT116 cells. Cells were incubated overnight with monensin, subsequently labeled using propidium iodide (PI) and their DNA content monitored by flow cytometry.

**Supplementary Table S5.** Analysis of phosphorylated amino acid residues in  $\beta$ -catenin. Beta-catenin precipitated from SW480 and HCT116 was subjected to the LC-MS/MS analysis. Cells were treated overnight with 5  $\mu$ M monensin or DMSO. The numbers indicate the probability (%) and the ion score for each detected modification. The probability and the ion score was calculated using PhosphoRS software and Mascot database search engine, respectively. Phosphorylation with the ion score  $\geq 43$  were considered as significant; n.d., not detected.

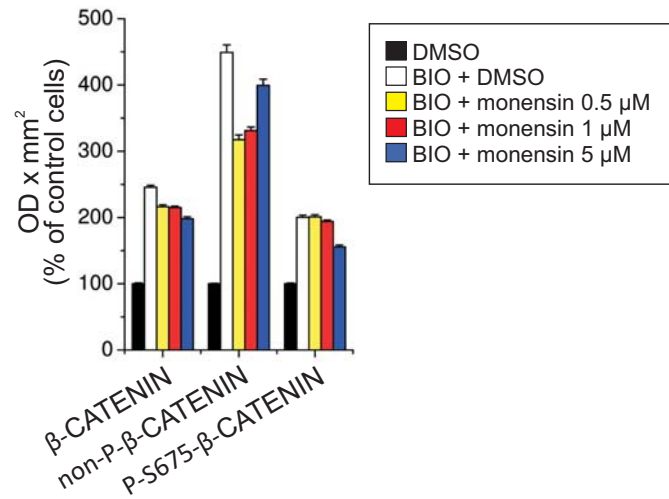


# Supplementary Figure S1

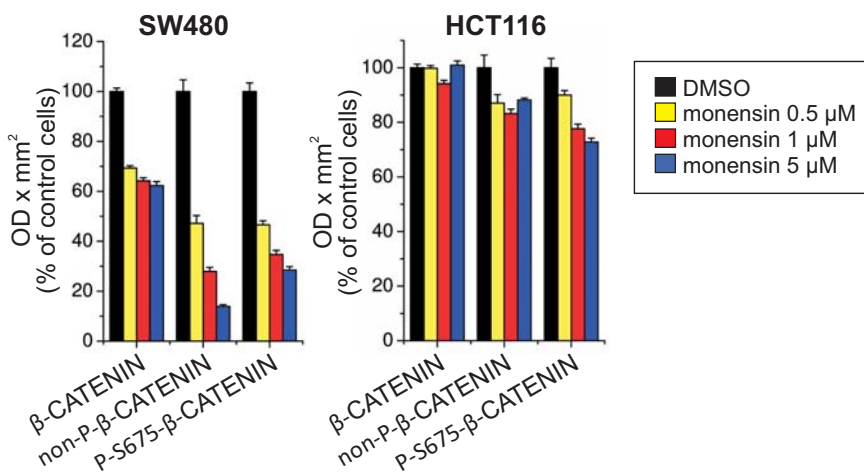
**A**



**B**

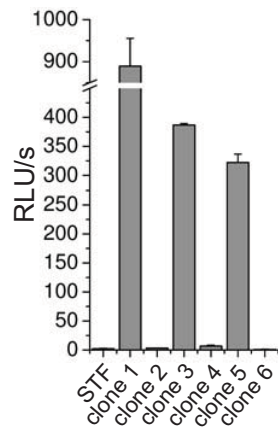


**C**

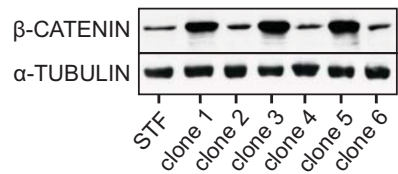


# Supplementary Figure S2

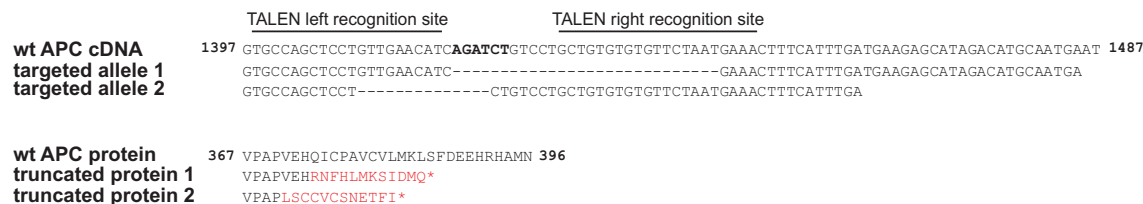
A



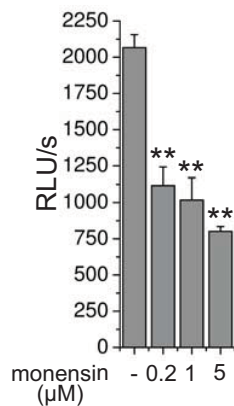
B



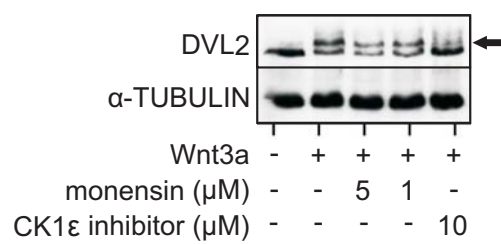
C



D



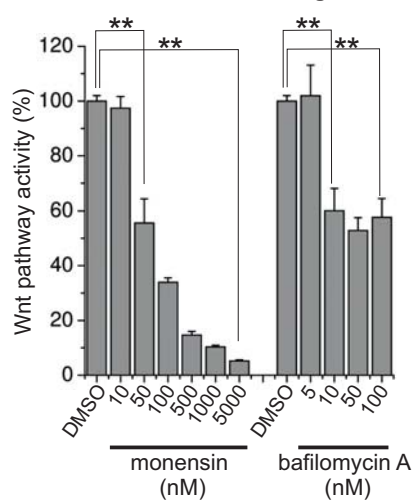
## Supplementary Figure S3



# Supplementary Figure S4

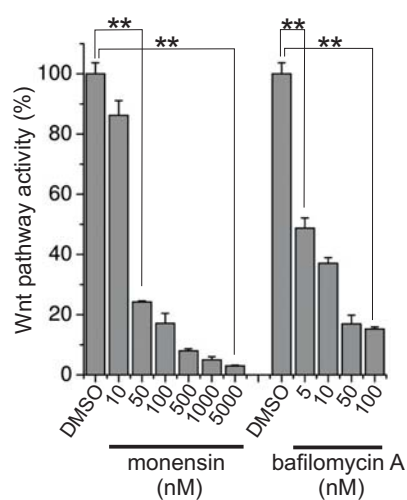
**A**

The Wnt pathway activation:  
recombinant Wnt3a ligand



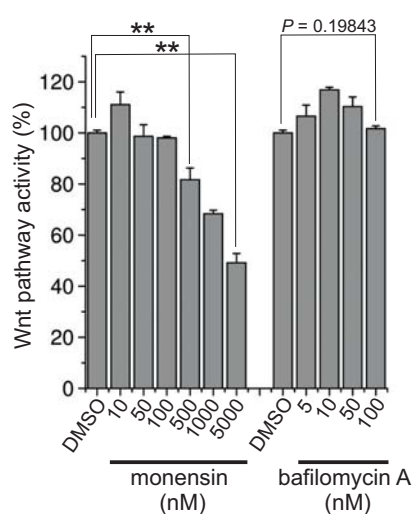
**B**

The Wnt pathway activation:  
ectopic expression of Wnt1



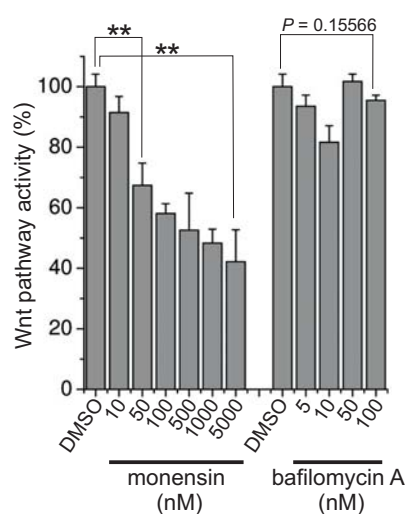
**C**

The Wnt pathway activation:  
ectopic expression of  $\Delta$ N-LRP6



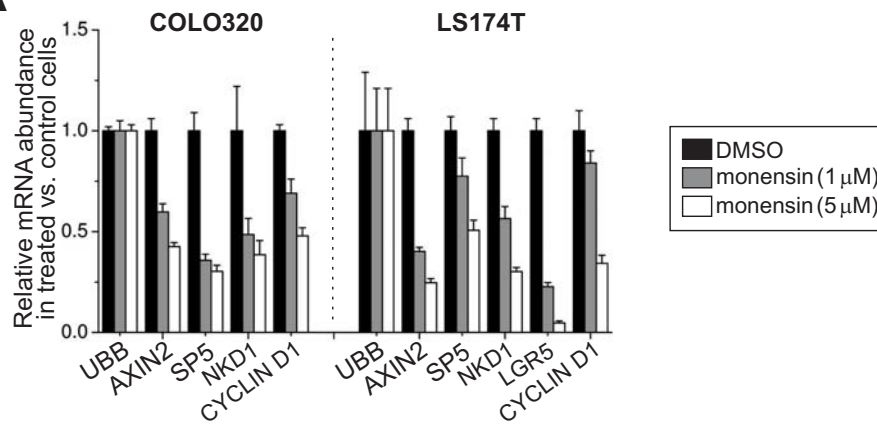
**D**

The Wnt pathway activation:  
ectopic expression of  $\beta$ -catenin

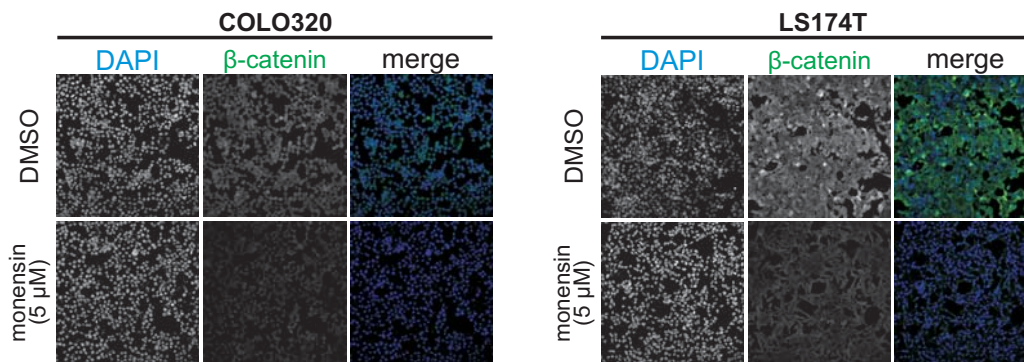


# Supplementary Figure S5

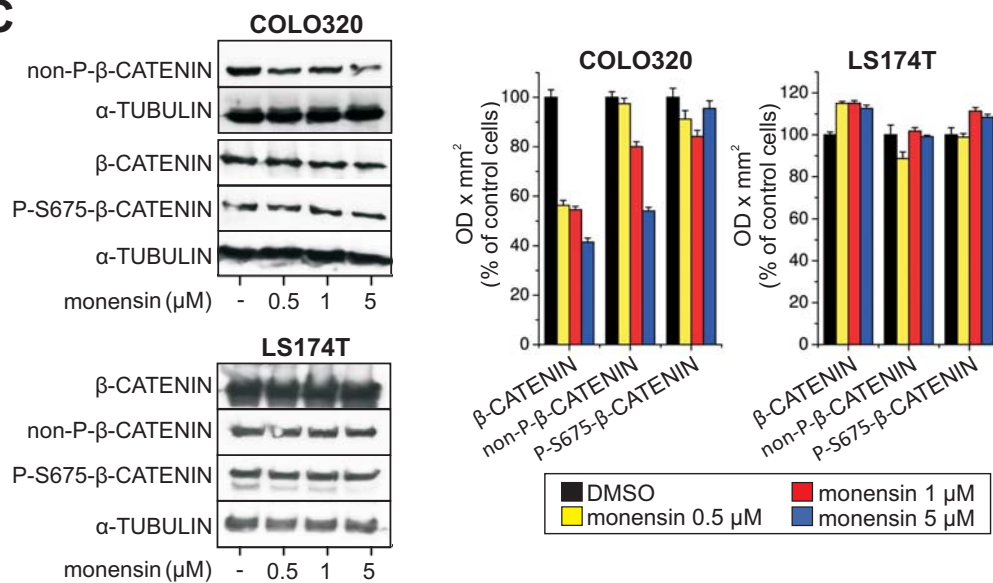
**A**



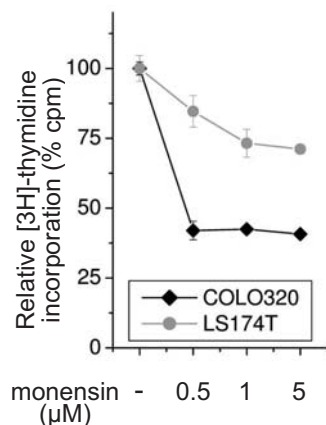
**B**



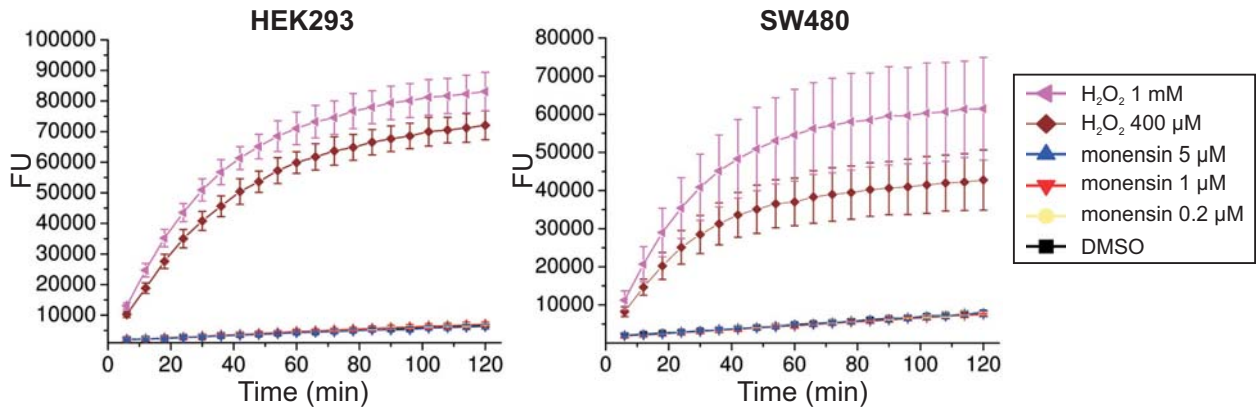
**C**



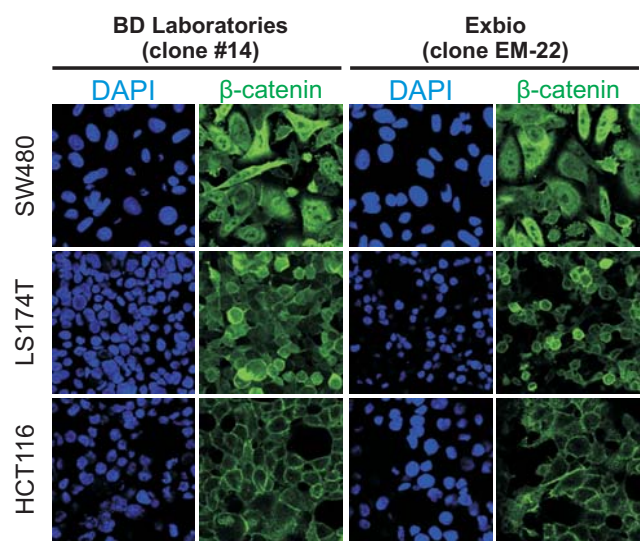
**D**



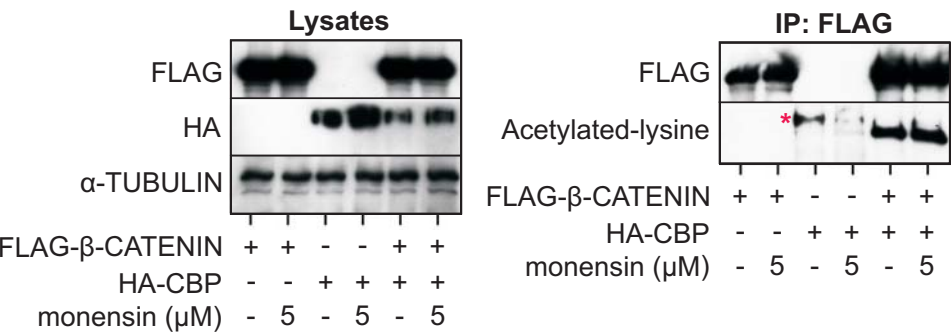
# Supplementary Figure S6



Supplementary Figure S7



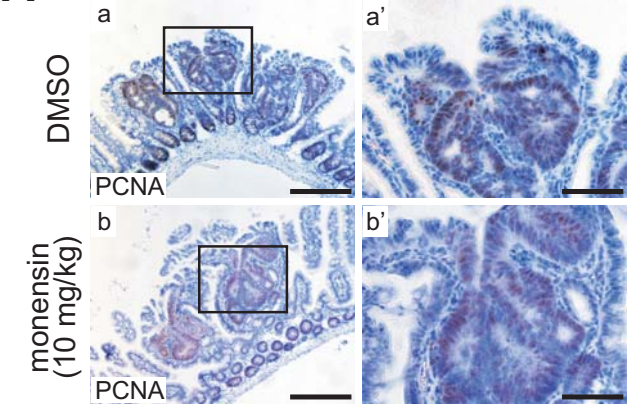
# Supplementary Figure S8



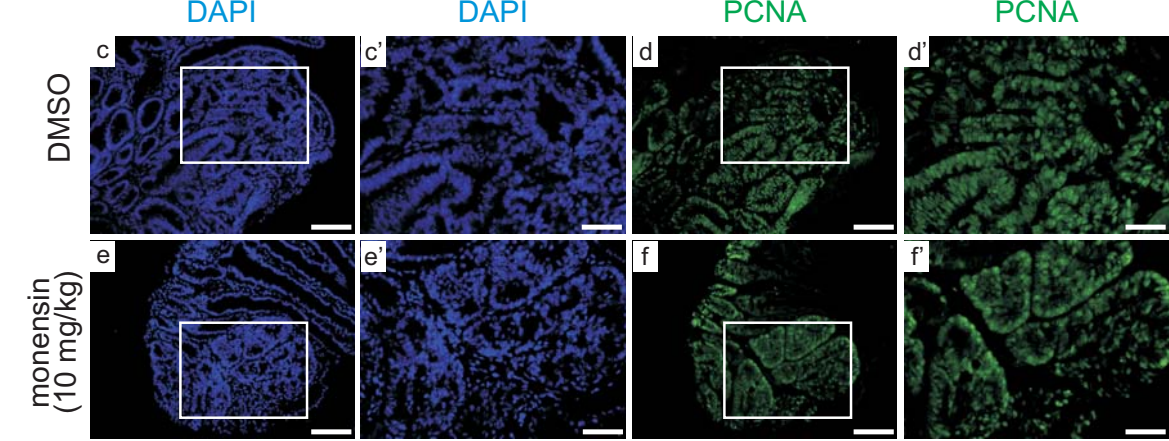


Supplementary Figure S9

A



B



C

